J-Researchers

Journal of Civil Engineering Researchers

Journal homepage: www.journals-researchers.com

Evaluation of Shape Memory Alloys in the Performance of Reinforced Concrete Frames under Near-Fault Earthquakes

Seyed Ahmad Mazloum,[a] Mahdi Mashhadiyan,[a,*] Elham Rajabpour,[b]

[a] *Department of Civil Engineering, Ramsar Branch, Islamic Azad University, Ramsar, Iran*

[b] *Department of Civil Engineering, Chalous Branch, Islamic Azad University, Chalous, Iran*

ABSTRACT

This study investigates and compares the performance of reinforced concrete buildings containing SMA bars and steel bars as longitudinal reinforcement of column. The use of this type of material is to reduce permanent deformation in the structure due to the reversible properties of these materials. First, a laboratory specimen of a reinforced concrete column with shape memory alloy bars was modeled in the OPENSEES software and the modeling method was validated. Then, 3- and 5-story concrete frames, in two states, reinforced with steel bars and SMA bars, under nonlinear static and nonlinear time history analyses with near-fault records were analyzed. The results of the time history analyses showed that, although the use of SMA bars significantly reduces the residual deformation of the structure, it does not show a significant effect on reducing the maximum displacement of the structure. The maximum rotational deformation of columns in frames with SMA bars is greater than of frames with steel bars. However, SMA bars have greatly reduced the permanent rotational deformation of columns and reduced it to zero. The maximum drift of floors in frames with SMA bars increases slightly. The permanent drift of the structure in frames with SMA bars is significantly reduced.

ARTICLE INFO

Received: July 14, 2024
Accepted: August 20, 2024

Keywords:
Concrete Frames
Nonlinear Static Analysis
Time History Dynamic Analysis
Shape Memory Alloy
Seismic Performance

DOI: 10.61186/JCER.6.4.1
DOR: 20.1001.1.22516530.1399.11.4.1.1

1. Introduction

During an earthquake, heavy structures, especially concrete structures, are subjected to significant forces due to their large mass [1,2]. The ways to dissipate the energy imposed on structures during an earthquake without destroying the stability of the structure are important. One of the ways to reduce the concrete structures damage is to use shape memory alloys (SMA) [3,4,5]. These materials are smart metals that have two different crystal structures, one of which is stable at high stresses and the other at low stresses. This reversible phase transformation has led to the emergence of special mechanical properties in them, which can improve the seismic performance of structures.

Shape memory alloys (SMAs) are a class of materials that have unique properties, including Young's modulus-temperature relations, shape memory effects, superelastic effects, and high damping characteristics [6]. Superelastic

* Corresponding author. Tel.: +98-911-196-2921; e-mail: mahdi.mashhadiyan@gmail.com.

shape memory alloys (SMAs) have the ability to undergo large deformations and recover all plastic deformations upon unloading. Their utilization in steel structures can significantly reduce seismic residual deformations, which will facilitate post-seismic retrofitting [7]. Experimental results by Sharabash & Andrawes, 2009 showed that the SMA braced frame could withstand several strong earthquakes with very limited capacity degradation [8]. The investigations by Abdulridha et al., 2013 and Abraik & Youssef, 2018 demonstrate the superior seismic performance of superelastic SMA RC as compared to steel RC. The results show that the crack widths and crack spacing were larger in the SMA beams; however, upon removal of load, the crack openings were recovered, Energy dissipation was lower in the SMA beams [9,10]. The results by Nikbakht et al., 2015 indicate that in high seismicity zones, bridge columns with SMA bars have a superior performance against earthquake loading [11]. Recent studies showed that concrete confinement using shape memory alloy (SMA) spirals is a promising technique for seismic retrofitting of reinforced concrete columns that lack flexural ductility [12]. Test results by Jung et al., 2018 show that SMA confinement is highly effective in mitigating the seismic damage and improving the seismic performance of retrofitted RC columns, subjected to strong earthquakes [13]. The analyses by Cortés-Puentes & Palermo, 2017 showed that the SMA braces can improve the lateral strength capacity, energy dissipation, and re-centering of reinforced concrete shear walls, while reducing strength and stiffness degradation associated with shear-related damage [14]. Elbahy, 2019 investigated the seismic performance of RC frames retrofitted using external superelastic SMA bars and compared to the behaviour of a regular steel RC frame structure. Analysis results show improved seismic performance for the retrofitted frames as compared to the original steel RC frame. This improvement was represented by lower level of damage at the same earthquake intensity and increased seismic capacity [15].

In this study, the effectiveness of shape memory alloys as longitudinal bars to improve the flexural performance of reinforced concrete beams and columns has been investigated. For this purpose, the performance of reinforced concrete frames with columns equipped with shape memory alloys and conventional ones has been evaluated.

2. Shape Memory Alloys

In general, two distinct behaviors can be defined for shape memory materials:

- Shape memory effect: When these materials are in the Martensite state, after applying stress and reaching a nonlinear state and creating residual strain by unloading, the residual strain of the material can be eliminated by applying temperature and the material will return to its original state [16].
- Superelastic behavior: Another important property of these materials that has attracted attention in civil engineering is superelastic behavior. This means that a sample of shape memory materials which is initially in the austenite state, upon applying stress, is converted to a less symmetrical Martensite state with lower stiffness. This behavior will cause nonlinear behavior. If the structure is unloaded at this time, the structure will return to the initial point in a path other than the loading path and no residual strain will be created [16].

3. Modeling

3.1. Structural Specifications

In this study, two 3- and 5-story buildings are modeled with steel bars in the beam, and in order to compare the performance, the columns of each of these buildings are modeled separately with steel bars and with SMA bars. The specifications of the buildings are as follows:

Each building has four spans in the X direction and three spans in the Y direction. The length of all spans is 5 meters and the height of the floors is 2.3 meters. The lateral load-bearing system of the building is a reinforced concrete frame. The connection of the column feet to the foundation is modeled as a bracket and the foundation of the structure is assumed to be rigid. The P-Δ effect is considered for the columns. The dead load applied to the floor of the floors is 550 kg/m^2 and the live load applied is 200 kg/m^2. The nodes at each floor level are interconnected in such a way that they can represent the behavior of a rigid roof. Concrete with a strength of 25 MPa has been used. The yield strength of steel bars and SMA bars has been considered to be 400 MPa. The modeling and cross-sectional characteristics of columns in the 3-story and 5-story frames are presented in Figure and Table 1.

The period of rotation obtained from 3- and 5-story frames in two cases including steel rebar and SMA rebar is presented in Table 2.

3.2. Selection of accelerograms and their scaling

Using nonlinear time history analysis in the OPENSEES software, the response of the structure is obtained as a function of time during the seismic event. To perform such an analysis, the nonlinear behavior of the materials is modeled and the accelerogram is defined.

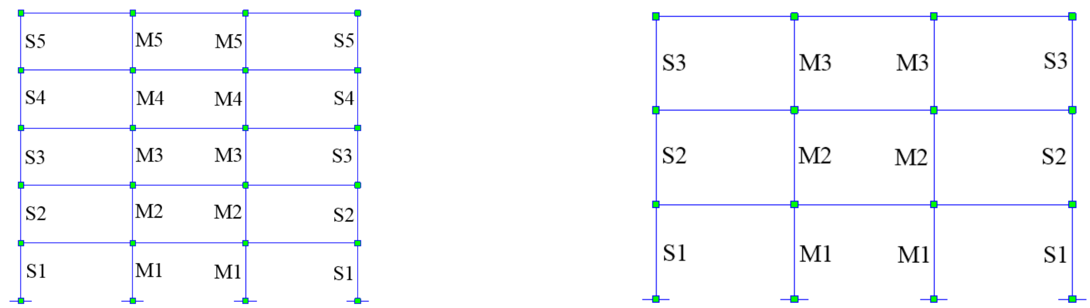

Figure 1: Modeling frame view

Table 1

Column cross-section specifications in 3- and 5-story frames

3-Storey					5-Storey				
Frame sections	b (mm)	h (mm)	Beams reinforced with steel bars		Frame sections	b (mm)	h (mm)	Beams reinforced with steel bars	
			ρs	ρs				ρs	ρs
S1	400	400	1.37	1.51	S1	450	450	1.59	1.73
S2	350	350	1.15	1.35	S2	450	450	1.00	1.00
S3	350	350	1.59	1.66	S3	400	400	1.00	1.00
M1	400	400	1.39	1.57	S4	400	400	1.00	1.00
M2	350	350	1.33	1.47	S5	400	400	1.10	1.06
M3	350	350	1.00	1.09	M1	450	450	1.76	2.11
---	---	---	---	---	M2	450	450	1.00	1.00
---	---	---	---	---	M3	400	400	1.21	1.28
---	---	---	---	---	M4	400	400	1.00	1.00
---	---	---	---	---	M5	400	400	1.00	1.00

Table 2

Period and frequency

Building	3 floors with steel rebar	3 floors with SMA rebar	5 floors with steel rebar	5 floors with SMA rebar
Period	0.84	0.79	1.15	1.08

To select the accelerograms and determine their characteristics and distance from the fault, is applied the set of records classified in FEMA P695, which was presented in 2009 under the title "Measurement of Building Seismic Performance Factors". For this study, seven near-fault earthquake records are considered according to Table 3.

The soil type, fault type, and distance from the epicenter for the near-fault accelerometer set are as follows. The selected earthquakes are related to soil type D according to the NEHRP standard. In the time history analysis method, the structural analysis is performed by giving the effect of ground acceleration as a function of time, at the base level of the building, and using conventional structural dynamics calculations. To achieve this goal, it is necessary to select at least three pairs of accelerometers belonging to the horizontal components of three different earthquakes recorded to satisfy the design earthquake conditions and in which the magnitude, distance from the fault, and the mechanism of the seismic source are considered.

3.3. Validation

Nakashoji et al. in 2014 tested a reinforced concrete column with a circular cross-section and a scale of one-third. The column diameter and height was selected 457 mm and 1.57 m, respectively. Sixteen SMA bars with a diameter of 13 mm were used for longitudinal reinforcement. Concrete with a strength of 47.5 MPa was used in this test [17].

Table 3

Earthquake name and station for the set of near-fault accelerograms

ID NO.	Earthquake		
	M	Year	Name
1	7.1	1999	Duzce
2	6.8	1990	Gazli
3	6.5	1979	Imperial
4	6.8	1985	Nahanni
5	6.9	1989	Loma
6	7.0	1992	Cape
7	6.7	1994	Northridge

Numerical modeling was performed in the OPENSEES software. In concrete modeling, nonlinear behavior of materials was considered. The well-known Kent & Park model was used to define the behavior curve of uniaxial concrete. The relationship of this model is as follows:

$$\sigma_c = f_c' \times \left[2\left(\frac{\varepsilon_c}{\varepsilon_c'}\right) - \left(\frac{\varepsilon_c}{\varepsilon_c'}\right)^2\right] \quad (1)$$

In this relation, σ_c and ε_c are the compressive stress and strain, respectively, f_c' and ε_c' are the compressive strength of the unconfined concrete cylindrical specimen and its corresponding strain, respectively.

In Figure 3, the base-drift shear curve obtained from the experiment is plotted next to the base-drift shear curve obtained from the OPENSEES model. According to the curves in Figure 3, the OPENSEES model was able to simulate the behavior of the reference specimen in an acceptable manner. The stiffness (initial slope) of both graphs coincided and the strength of the finite element model was able to predict the strength of the reference model with a difference of less than 5%.

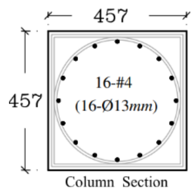

Figure 2: Column cross-section characteristics

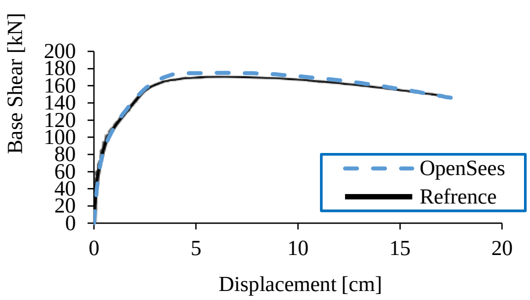

Figure 3: Base shear-drift curve obtained from the experiment next to the base shear-drift curve obtained from the OPENSEES model

4. Time history analysis

4.1. Three-story building

Time history analysis of the three-story model was performed in two cases of steel rebar and alloy rebar using seven different earthquake records. In Figure 4, the time history curve related to the base shear and roof floor displacement of the three-story frame under the effect of a two-three earthquake is plotted. The green graph is for the frame with steel rebars and the blue graph is for the frame with SMA rebars in the column.

According to Figure 4, the maximum base shear applied to steel bars is greater than that of SMA bars and the maximum displacements are not much different between the two types of bars. In Figure 5, the lateral displacement curve of the floors (drift) in a three-story building with a column with steel bars and SMA bars under the effect of a two-magnitude earthquake is plotted next to each other. According to the obtained graphs, the maximum drift in both structures is similar to each other and the overall behavior of the two structures is not much different. However, the permanent drift of the structure with SMA bars is less compared to the structure with steel bars.

The maximum rotation of beams and columns at different floors of a three-story frame is plotted in Figure 6 (a) and (b), respectively. The blue graph is for the frame with steel rebar in the column and the orange graph is for the frame with SMA rebar in the column.

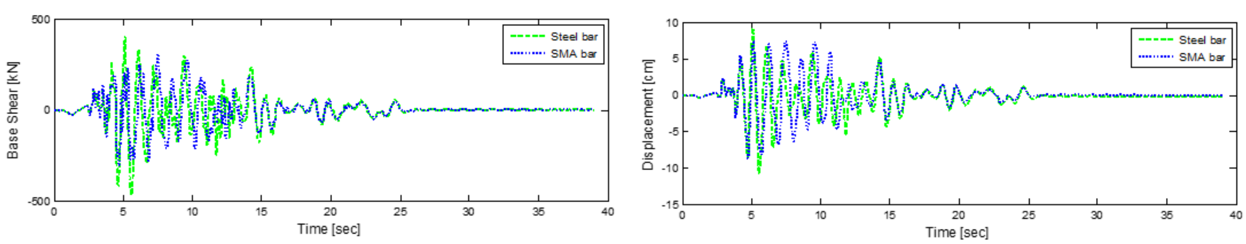

Figure 4: Three-story frame under the influence of Duzce earthquake (a) Base shear (b) Roof displacement

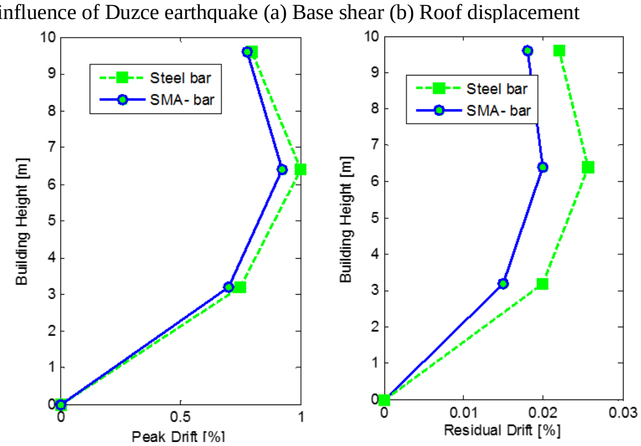

Figure 5: Drift curve of floors in a three-story building with a column with steel rebar and SMA rebar

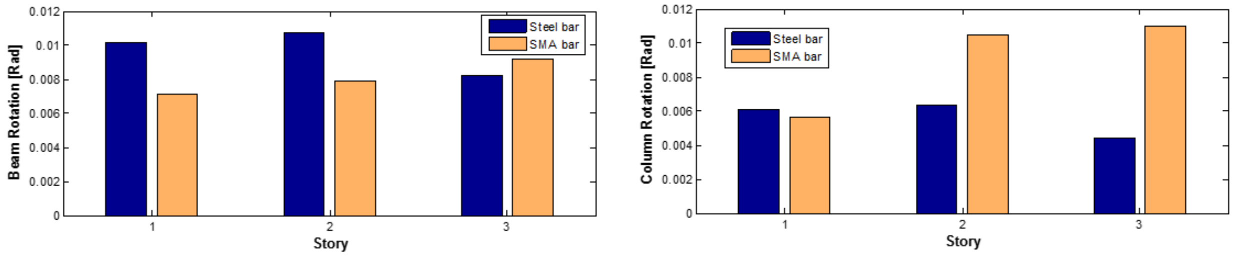

Figure 6: Maximum rotation at different floors (average of seven records) (a) Beam rotation (b) Column rotation

According to figure 6, the use of SMA rebar has reduced the rotation of beams and the use of SMA rebar has increased the rotation of columns.

4.2. Five-story building

In Figure 7-9, the time history curve of the base shear of the five-story frame under the effects of the Duzce, Northridge, and Imperial earthquakes is plotted and the difference in the performance of steel rebar and SMA in these three types of earthquakes is clearer. As shown in the figure, the maximum base shear applied to steel rebar is higher.

Figure 10(a) and (b) show the time history curves of the roof displacement of the five-story frame under the Northridge and Imperial earthquakes, respectively. The steel-reinforced column (green curve) has undergone permanent displacement and its final displacement is not zero and in fact the building has not returned to its original state. But, the building with the SMA-reinforced column has returned to its original state.

Figure 11 shows the lateral displacement curve of the floors (drift) in the five-story building with the steel-reinforced column and the SMA-reinforced column under the Imperial earthquake. According to the obtained graphs, the maximum drift in both structures is similar to each other and the overall behavior of the two structures is not much different, but the permanent drift of the structure with the SMA-reinforced has decreased sharply and the structure has returned to its original state, while the permanent drift has occurred in the steel-reinforced structure.

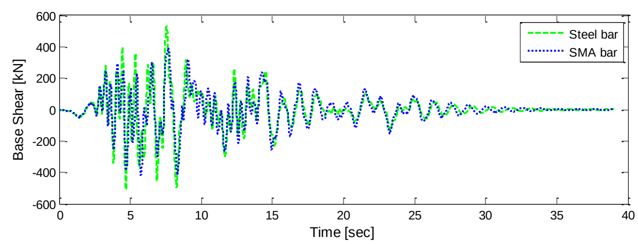

Figure 7: Base shear of the Duzce earthquake

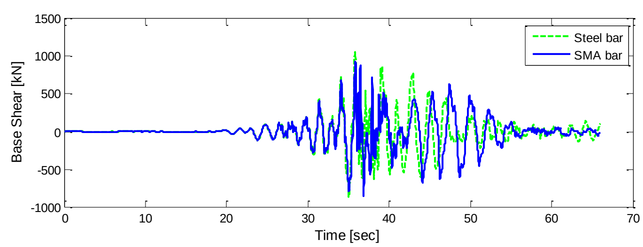

Figure 8: Base shear of the Northridge earthquake

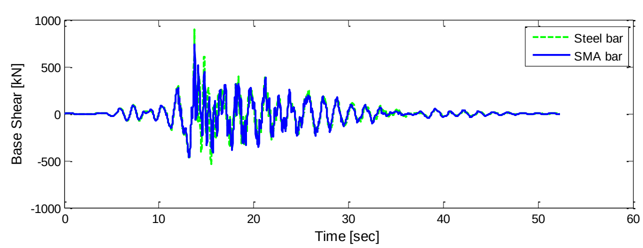

Figure 9- Base shear of the Imperial earthquake

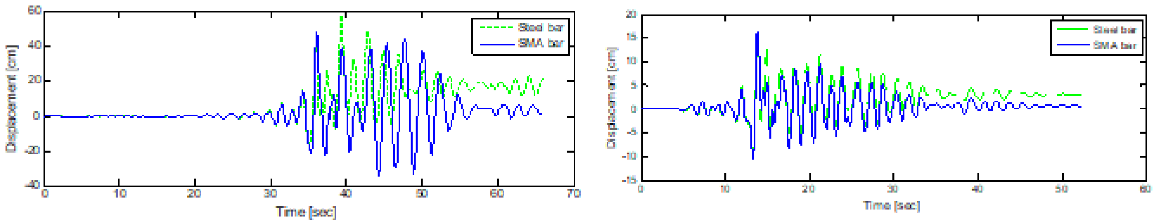

Figure 10- Roof displacement (a) Northridge earthquake (b) Imperial earthquake

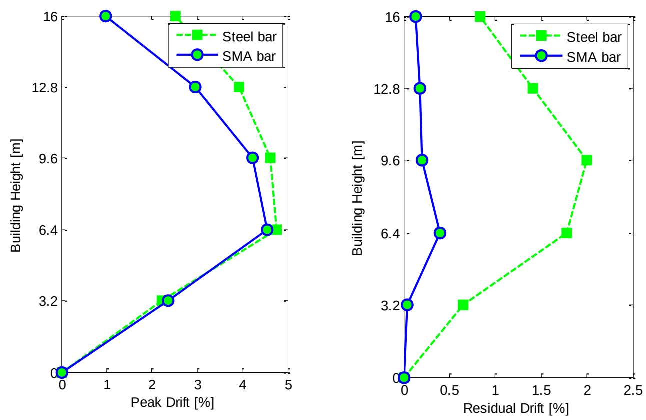

Figure 11- Lateral displacement of floors (drift) in a five-story building under Imperial earthquake

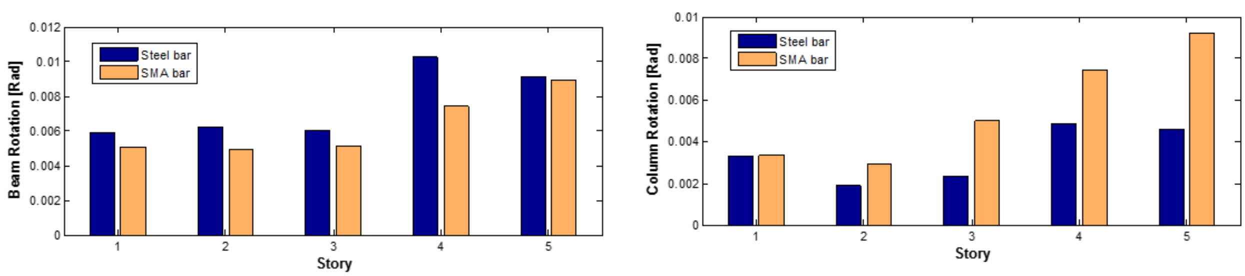

Figure 12- Maximum rotation at different floors (average of seven records) (a) Beam rotation (b) Column rotation

The maximum rotation of beams and columns in different floors of the five-story frame are plotted in Figure 12 (a) and (b), respectively. According to this figure, the use of SMA rebar has reduced the rotation of beams and increased the rotation of columns.

5. Investigation of the effect of the ratio of shape memory alloy

In order to investigate the effect of the ratio of shape memory alloy, a 5-story frame with an average rebar ratio of 1.4% and 2.1% for columns was analyzed using pushover analysis and the deformation of beams and columns in these two cases was compared. According to Figure 13, the maximum frame capacity in the model with an average rebar ratio of 2.1% was obtained as 770 kN, which shows a 15% increase compared to the model with an average rebar ratio of 1.4%. According to Figure 14, in the model with an average rebar ratio of 2.1%, a slight increase in the rotation of beams and a slight decrease in the rotation of columns occurred.

6. Conclusion

This study investigates the performance of reinforced concrete buildings with SMA bars in columns under near-fault earthquakes. For this purpose, two three-story and five-story buildings were considered. These buildings were analyzed once using steel bars and once using SMA bars in seven near-fault accelerograms. The following results is obtained:

- The performance of SMA bars did not differ significantly compared to steel bars in reducing the maximum displacements of the structure and their effectiveness was almost similar. However, the use of SMA bars has greatly reduced the permanent deformation of the structure.

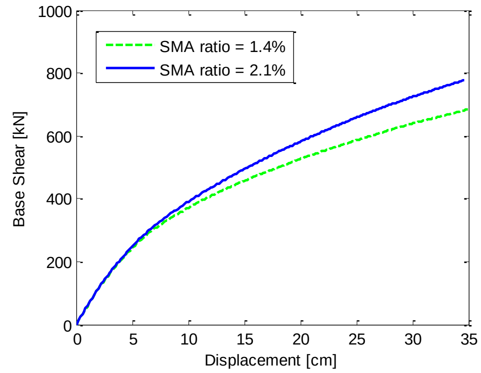

Figure 13 : Pushover curve

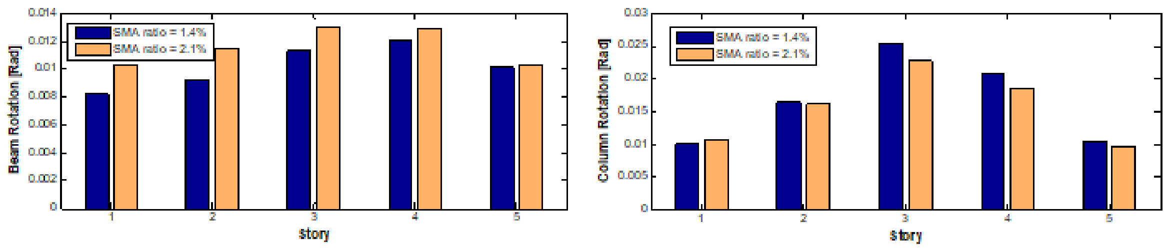

Figure 14 : Maximum rotation at different floors (average of seven records) (a) Beam rotation (b) Column rotation

- In frames with SMA bars in columns, the maximum rotational deformation of the columns was greater than that of frames with steel bars. However, SMA bars have greatly reduced the permanent rotational deformation of the columns and brought them to zero.
- The maximum lateral displacement or maximum drift of the floors in frames with SMA bars has slightly increased. However, the permanent drift of the structure in frames with SMA reinforcement is greatly reduced. This is due to the elastic recovery of strain in SMA materials, which reduces the permanent deformation of the structure.

References

[1] Jha, Nitya Nand, Rohit Kumar Singh, and Sushila Sharma. "Behaviour and design of a (G+ 5) multi storey framed structure under different loading condition." Asian Journal of Civil Engineering 25.7 (2024): 5293-5305. https://doi.org/10.1007/s42107-024-01113-w

[2] Anas, S. M., Mehtab Alam, and Messaoud Saidani. "Prediction of impact response of square reinforced concrete (RC) slab with square/circular opening under drop-weight impact using FEM simulation." Asian Journal of Civil Engineering 25.2 (2024): 2189-2208. https://doi.org/10.1007/s42107-023-00903-y

[3] Elroby, Shaimaa A., et al. "Experimental and machine learning-based model for large-scale reinforced concrete shear walls strengthened with CFRP sheets and shape memory alloys." Asian Journal of Civil Engineering (2024): 1-19. https://doi.org/10.1007/s42107-024-01135-4

[4] Fawzy, Khaled, et al. "Overview of the punching capacity of the flat slab under reversed cyclic loading and methods of improvement." Asian Journal of Civil Engineering 25.3 (2024): 2641-2652. https://doi.org/10.1007/s42107-023-00934-5

[5] Kiani, Mahdi, and Hamed Enayati. "Evaluation of a nonlinear TMD seismic performance for multi-degree of freedom structures." Asian Journal of Civil Engineering 25.2 (2024): 1395-1412. https://doi.org/10.1007/s42107-023-00850-8

[6] DesRoches, R., and B. Smith. "Shape memory alloys in seismic resistant design and retrofit: a critical review of their potential and limitations." Journal of earthquake engineering 8.3 (2004): 415-429. https://doi.org/10.1080/13632460409350495

[7] Sultana, Papia, and Maged A. Youssef. "Seismic performance of steel moment resisting frames utilizing superelastic shape memory alloys." Journal of Constructional Steel Research 125 (2016): 239-251. https://doi.org/10.1016/j.jcsr.2016.06.019

[8] Sharabash, Alaa M., and Bassem O. Andrawes. "Application of shape memory alloy dampers in the seismic control of cable-stayed bridges." Engineering Structures 31.2 (2009): 607-616. https://doi.org/10.1016/j.engstruct.2008.11.007

[9] Abdulridha, Alaa, et al. "Behavior and modeling of superelastic shape memory alloy reinforced concrete beams." Engineering Structures 49 (2013): 893-904. https://doi.org/10.1016/j.engstruct.2012.12.041

[10] Abraik, Emad, and Maged A. Youssef. "Seismic fragility assessment of superelastic shape memory alloy reinforced concrete shear walls." Journal of building engineering 19 (2018): 142-153. https://doi.org/10.1016/j.jobe.2018.05.009

[11] Nikbakht, Ehsan, et al. "Application of shape memory alloy bars in self-centring precast segmental columns as seismic resistance." Structure and Infrastructure Engineering 11.3 (2015): 297-309. https://doi.org/10.1080/15732479.2013.876056

[12] Chen, Qiwen, and Bassem Andrawes. "Cyclic stress–strain behavior of concrete confined with NiTiNb-shape memory alloy spirals." Journal of Structural Engineering 143.5 (2017): 04017008. https://doi.org/10.1061/(ASCE)ST.1943-541X.0001728

[13] Jung, Donghyuk, James Wilcoski, and Bassem Andrawes. "Bidirectional shake table testing of RC columns retrofitted and repaired with shape memory alloy spirals." Engineering structures 160 (2018): 171-185. https://doi.org/10.1016/j.engstruct.2017.12.046

[14] Cortés-Puentes, W. Leonardo, and Dan Palermo. "SMA tension brace for retrofitting concrete shear walls." Engineering Structures 140 (2017): 177-188. https://doi.org/10.1016/j.engstruct.2017.02.045

[15] Elbahy, Yamen Ibrahim, Maged A. Youssef, and M. Meshaly. "Seismic performance of reinforced concrete frames retrofitted using external superelastic shape memory alloy bars." Bulletin of Earthquake Engineering 17 (2019): 781-802. https://doi.org/10.1007/s10518-018-0477-7

[16] Brinson, L. Catherine. "One-dimensional constitutive behavior of shape memory alloys: thermomechanical derivation with non-constant material functions and redefined martensite internal variable." Journal of intelligent material systems and structures 4.2 (1993): 229-242. https://doi.org/10.1177/1045389X9300400213

[17] Nakashoji, Brian A. Seismic performance of square nickel-titanium reinforced ECC columns with headed couplers. University of Nevada, Reno, 2014.